JETIR.ORG ISSN: 2349-5162 | ESTD Year : 2014 | Monthly Issue
JOURNAL OF EMERGING TECHNOLOGIES AND INNOVATIVE RESEARCH (JETIR)
An International Scholarly Open Access, Peer-reviewed, Refereed Journal

The dynamic's response to the flexibility of the diaphragm The way unreinforced masonry walls behave in Unplanar Bending

[1] Hiral D.Rathod, [2]K R Ghadge

[1] Post Graduate Student,[2]Associate Professor,

[1]Civil Engineering Department,

[1]Sanmati college Of Engineering Washim ,India

Abstarct: This study examines the dynamic behaviour of historic, unreinforced masonry buildings' exterior walls made of flexible diaphragms that are bent out of plane. Dynamic analyses using a streamlined two-degrees-of-freedom model (2DOF) have been used to investigate the effect of diaphragm flexibility on the displacement capacity and demand of walls in out-of-plane bending. The wall has been modelled as an assembly of two rigid bodies constrained at the top by a spring and joined by an intermediate hinge. The damping has been modelled by adding the coefficient of restitution. The 2DOF system's equations of motion have been calculated and integrated in time. A set of walls have undergone dynamic analysis using recorded accelerogram inputs and a gaussian impulse. In order to compare the responses of the wall that is simply supported and the wall that has an elastic spring at the top.

Keywords: Out-of-Plane Bending, Unreinforced Masonry, Dynamic Analysis, Flexible Diaphragms

1.INTRODUCTION

Out-of-plane wall collapses of old unreinforced masonry buildings are frequent and extremely dangerous, even in terms of human life loss, according to observations of the seismic damage done to those structures. As a result of the poor links between the many structural elements that characterise historical buildings, local collapses frequently occur before global ones. Single components of a building can split from the rest of it during earthquakes and frequently behave as completely independent structural components. Therefore, it is crucial to research how such systems behave, and in recent years, several academics have done just that. Various methods have been suggested, including static, kinematic, or dynamic analysis, elasto-plastic, no-tension, or stiff models, however there have only been a small number of experimental experiments. been emphasised on the most basic failure mechanisms (parapet wall or merely supported wall) because to their easier replication and understanding. However, only recently have some analytical and experimental studies (Doherty, 2000; Doherty et al., 2002; Griffith et al., 2003; Griffith et al., 2004; Lam et al., 2003; Sorrentino, 2003; Sorrentino, 2008) highlighted the necessity of dynamic analysis in order to understand the actual behaviour of walls in actual situations. Housner's work (Housner, 1963) served as the foundation for the dynamic studies on the They emphasised that out-of-plane collapses of walls are mostly caused by an excessive displacement demand as opposed to force or acceleration demand, and that static approaches, which concentrate on comparing forces and resistance, are therefore unable to capture some special dynamics-related characteristics. Since diaphragms were assumed to be rigid, the complexity of the dynamic issue and the number of degrees of freedom were reduced in nearly all previous publications that explored simpler hypotheses about how the wall interacts with the rest of the

building. When the diaphragms cannot be thought of as rigid, as they are in most historical buildings, the inputs to the out-of-plane walls at adjacent floors have different amplitude, phase, and duration. This implies that the path of the seismic action from the ground to the out-of-plane walls implies a filtering effect of the shear walls and diaphragm response. content of frequency. Instead of using the standard single-degree model in this situation, numerous degrees of freedom must be taken into account. Simsir (2004) found that there are very few studies that explicitly consider the impact of diaphragm flexibility on displacement capacity and demand. In order to examine the dynamic out-of-plane behaviour of a single wall with the flexible diaphragm hypothesis, a simple 2DOF model has been constructed by extending various formulations suggested by other authors (Doherty, 2000; Sorrentino, 2003; Simsir, 2004). The major findings are given after the wall's motion equations were generated and a technique for their numerical integration was created.

2.MODEL DESCRIPTION

To examine the dynamic out-of-plane behaviour of a single wall with an intermediate hinge and a top elastic spring, a simplified 2DOF model has been built. The wall is described as an assembly of two rigid bodies, a lower and an upper half, each of which is free to rotate around the intermediate hinge, as illustrated in Fig. 1.1.

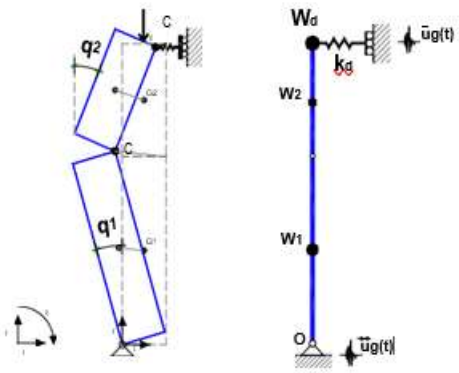

Fig.2.1 2DOF model of the wall in out-of –plane bending

In Fig. 2.1 W_1 and W_2 are the weights of the lower and upper part of the wall, W_d is the overburden load from the diaphragm, K_d is the translational stiffness of the spring at the top, that simulates the in- plane stiffness of the upper diaphragm and is considered perfectly elastic, q_1 e q_2 are the rotations, respectively of the lower and the upper portion of the wall related to the vertical axis, that have been assumed as independent variables. The intermediate hinge has been assumed at the mid-height of the wall and the load W_d is supposed to be applied at the middle of the thickness, in order to reproduce the hypotheses made by Doherty in his study on the simply supported wall (Doherty, 2000) and to compare the results obtained by Doherty with the ones of the present study.3.EQUATIONS OF MOTION

The Lagrange equations have been used to derive the equations of motion for the two degrees of freedom system, taking into account the kinetic energy resulting from the translation of the masses and the rotation of the two parts of the wall around their respective centroids as well as the potential energy resulting from the translational spring at the top and the gravitational loads' contribution. The aforementioned figures were computed under the presumption of slight displacements.

3.1.Geometric possible configurations

Due to the abrupt change in the point of rotation at the base and intermediate hinges, the equations of motion are extremely nonlinear. The passing from one condition to another is defined by an impact at the bottom or at the intermediate hinge connected with the shift of the centre of rotation (see Fig. 3.2). There are four different conditions, each described by four related sets of equations (see Fig. 3.1).

Every time q_1 passes through the zero, there is an impact at the bottom and a change of the centre of rotation (O to O' or O' to O): similarly, every time $q_1 = q_2$, there is an impact at the intermediate hinge

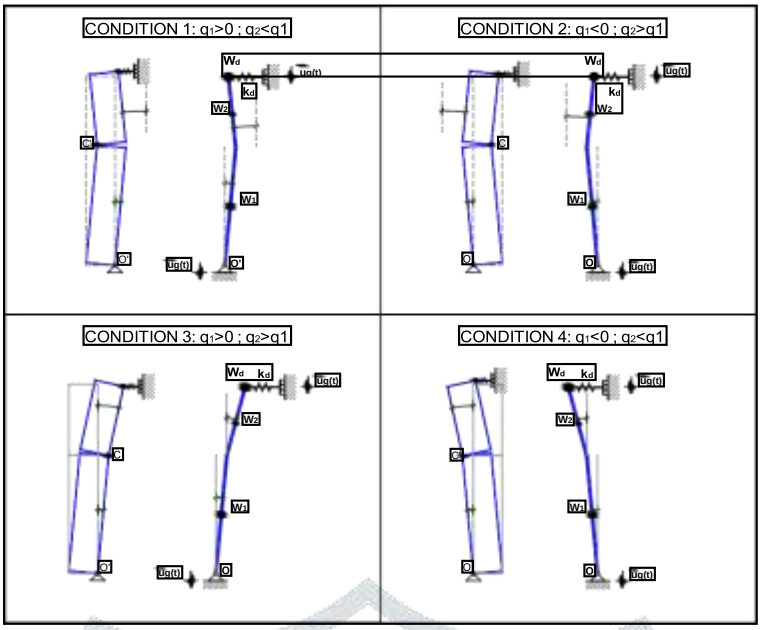

Fig 3.1 2Dfmodel of the wall in oyt-of-plane beding

3.2.Energy dissipation:

The equations of motion are as follows, assuming that h is the entire height of the wall, g is the acceleration of gravity, W1=W2 since the intermediate hinge is located at the midpoint of the wall, and that the clockwise rotations are positive:

$$\begin{bmatrix} m_{11} & m_{12} \\ m_{21} & m_{22} \end{bmatrix} \begin{bmatrix} \ddot{q}_1 \\ \ddot{q}_2 \end{bmatrix} + \begin{bmatrix} k_{11} & k_{12} \\ k_{21} & k_{22} \end{bmatrix} \begin{bmatrix} q_1 \\ q_2 \end{bmatrix} = \begin{bmatrix} p'_{eff,1}(t) + A_i \\ p'_{eff,2}(t) + B_i \end{bmatrix}$$

The coefficients of the mass matrix are reported in Eqn. 3.2:

$$\begin{cases} m_{11} = \left[\frac{W_1}{3} + \frac{W_d}{4}\right] \cdot \frac{h^2}{g} \\ m_{12} = m_{21} = \left[\frac{W_1}{8} + \frac{W_d}{4}\right] \cdot \frac{h^2}{g} \\ m_{22} = \left[\frac{W_1}{12} + \frac{W_d}{4}\right] \cdot \frac{h^2}{g} \end{cases}$$

The coefficients of the stiffness matrix are reported in Eqn. 3.3:

$$\begin{cases} k_{11} = \left[\frac{K_a \cdot h^2}{4} - \frac{3}{4} \cdot W_1 \cdot h - W_d \cdot \frac{h}{2}\right] \\ k_{12} = k_{21} = \frac{K_a \cdot h^2}{4} \\ k_{22} = \left[\frac{K_a \cdot h^2}{4} - W_1 \cdot \frac{h}{4} - W_d \cdot \frac{h}{2}\right] \end{cases}$$

The terms $p_{eff,1}(t)$ and $p_{eff,2}(t)$ represent the contribution due to the ground acceleration. They are reported in Eqn. 3.4:

$$\begin{cases} p'_{eff,1}(t) = -\ddot{u}_g \cdot \left[-3 \cdot W_1 - 2 \cdot W_d\right] \cdot \dfrac{h}{4 \cdot g} \\ p'_{eff,2}(t) = -\ddot{u}_g \cdot \left[-W_2 - 2 \cdot W_d\right] \cdot \dfrac{h}{4 \cdot g} \end{cases}$$

The terms A_i and B_i in Eqn. 3.1 are different in the four conditions: they are expressed in Eqn. 3.5, 3.6, 3.7, 3.8.

Condition 1 ($q_1>0$ and $q_2<q_1$):

$$\begin{cases} A_1 = -\dfrac{3 \cdot W_1}{2} \cdot b - W_d \cdot b \\ B_1 = \dfrac{1}{2} \cdot b + W_d \cdot \dfrac{b}{2} \end{cases}$$

Condition 2 ($q_1<0$ and $q_2>q_1$):

$$\begin{cases} A_1 = -\dfrac{3 \cdot W_1}{2} \cdot b - W_d \cdot b \\ B_1 = \dfrac{1}{2} \cdot b + W_d \cdot \dfrac{b}{2} \end{cases}$$

Condition 3 ($q_1>0$ and $q_2>q_1$):

$$\begin{cases} A_2 = +\dfrac{3 \cdot W_1}{2} \cdot b + W_d \cdot b \\ B_2 = -\dfrac{1}{2} \cdot b - W_d \cdot \dfrac{b}{2} \end{cases}$$

Condition 4 ($q_1<0$ and $q_2<q_1$):

$$\begin{cases} A_4 = +\dfrac{W_1}{2} \cdot b \\ B_4 = +\dfrac{W}{2} \cdot b + W_d \cdot \dfrac{b}{2} \end{cases}$$

4.NUMERICAL ALGORITHM

A variable step size Runge-Kutta integration method of fourth- to fifth-order, implemented in Matlab ODE-suite ODE45, has been employed in the development of an algorithm for the numerical integration of sets of equations of motion in the time domain. Each step of the numerical integration has been subjected to a local error control, with suitably low values of the relative tolerance RelTol and the absolute tolerance AbsTol (RelTol=10-5 and AbsTol=10-10), respectively. The abrupt change in the sign of the resisting moment of the weights W1 and W2 and of Wd about the effective centre of rotation at the bottom and intermediate hinges, which corresponds to the abrupt change in the hinge's position, causes the strong nonlinearity of the set of motion equations.

$$M_{q1} = \left| \frac{3}{4} \cdot W_1 \cdot h + W_d \cdot \frac{h}{2} \right| \cdot q_1 + A_i$$

$$M_{q2} = \left| \frac{W_1}{4} \cdot h + W_d \cdot \frac{h}{2} \right| \cdot q_2 + B_i$$

Eqn. 4.1 and Eqn. 4.2 present the expression of M_{q1} and M_{q2}: M_{q1} is the resisting moment about the bottom hinge O or O' (depending on the actual condition) of the self weight W_1 of the lower part of the wall and of the weights W_2=W_1 and W_d transferred from the upper to the lower part of the wall at the intermediate hinge C or C'; M_{q2} is the resisting moment about the intermediate hinge C or C'(depending on the actual condition) of the weights W_2 and W_d. A_i and B_i are presented in Eqn. 3.5, Eqn. 3.6, Eqn. 3.7 and Eqn. 3.8 and represent the resisting moments M_{q1} and M_{q2} when the independent variables q_1 and q_2 are zero.

The diagrams of Mq1 in the four conditions are shown in Fig. 4.1 (represented by the green and red continuous lines); the diagram of Mq1 in the hypothesis of the stiff behaviour of the wall is represented by the blue dotted line. The two purple and yellow lines represent the change from one condition to another at q1=0, following the Doherty studies' (Doherty, 2000) suggestion that the stiffness at this point be finite rather than infinite. The algorithm then follows these lines rather than the rigid behavior's blue lines. The values of q1 at the intersections of the diagrams of Mq1 in the four conditions with the line of finite stiffness are represented by the parameters -D12,1, -D34,1, D34,1, and D12,1. changes from condition 1 to condition 4 or from The vertical black dotted lines depict the impacts at the intermediate hinge, which occur when the ratios of 4 to 1 and from 2 to 3 or from 3 to 2 occur (q1=q2).

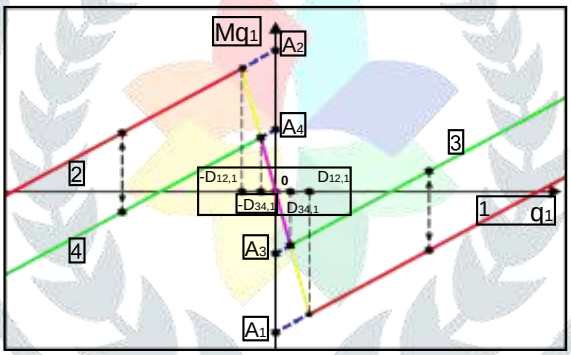

Fig.4.1 Resisting moment M_{q1} in the 4 conditions

Fig. 4.2 shows the diagrams of M_{q2} in the 4 conditions (red continuous lines): the couples of conditions 1 and 4, 2 and 3 have the same diagram. Similarly to the diagram of Fig. 4.1 an initial finite stiffness is assumed (purple dotted line). The parameters -$D_{12,2}$, $D_{12,2}$ are the values of q_2 at the intersections of the diagrams of M_{q2} in the 4 conditions with the line of finite stiffness. Transitions from conditions 1 or 4 to conditions 2 or 3 or from conditions 2 or 3 to conditions 1 or 4, corresponding to an impact at the intermediate hinge (q_1=q_2), are represented by the vertical black dotted lines, while transitions at q_1=0 do not cause any jump in the diagram.

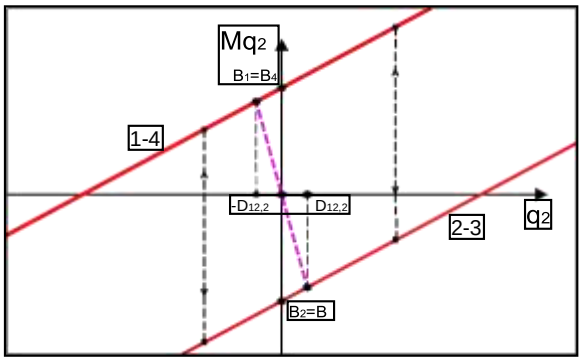

Fig 4.2 Resisting moment M_{q2} in the 4 conditions

equations of motion of the Eqn. 3.1 until the first event: the algorithm can detect the events at the target values of q_1 and q_2: the integration stops when the variable q_1 assumes the values $-D_{12,1}$, $-D_{34,1}$, 0, $D_{34,1}$, $D_{12,1}$ or when the variable q_2 assumes the values $-D_{12,2}$, $D_{12,2}$ or when $q_1 = q_2$. State variables identify the condition corresponding to each time step: the value of these variables at the event defines the condition before the event and allows the algorithm to decide which condition to assume afterwards and which line to follow in Fig. 3.1 and 3.2. Except for the impact for q_1=0, the values of the rotations q_1 and q_2 and the corresponding angular velocities after every event are the same detected at the event. These are the new initial conditions of the differential equations that the algorithm assumes in order to integrate the appropriate equations, depending on the effective initial geometrical configuration of the wall. For q_1=0, the rotations after the impact are the same as the ones before the impact, while the angular velocities of the lower and upper part of the wall are reduced by the restitution coefficient e_r<1.

5.RESULTS

To verify the numerical approach used in the present work and to compare Doherty's results to those obtained with the 2DOF model in the case of a very high value of stiffness of the top spring—in that case, the top and bottom absolute displacements of the wall tend to be equal and in phase—an algorithm for the integration of the equations of motion of the semi-rigid 1DOF model has been implemented. The experimental and analytical findings by Doherty indicated that the 1DOF model created in the present work was in good accord with those findings. dynamic studies with recorded accelerogram inputs and a gaussian distribution have been carried out on a group of walls, altering the stiffness Kd at the top values and researching its impact on the displacement demand. Both the 1DOF and the 2DOF models employ the same coefficient of restitution, er=0.86.

5.1.Set of walls

A set of 3 walls with different characteristics, in terms of maximum resisting force and ultimate displacement in the hypothesis of rigid behaviour (see Table 5.1 and Fig. 5.1) has been considered.
In Table 5.1 b is the thickness, h is the height, W is the self weight of the wall, □ is the ratio between W_d and W_1, R_{e1} is the rigid threshold resistance and Δ_u is the ultimate displacement, calculated following Doherty formulation (Doherty, 2000; Doherty et al., 2002).

Wall	b	h	□	W	$Re1$	Δ_u	$F0/W$	Δ_u/b
	[m]	[m]	[-]	[KN/m]	[KN/m]	[m]	[-]	[-]
1	0,15	2,5	0	6,622	1,192	0,150	0,180	1,000
2	0,15	2,5	0,5	6,622	1,639	0,138	0,248	0,917
3	0,15	2,5	1	6,622	2,086	0,131	0,315	0,875

Fig 5.1 set a considered wall

5.2.Semi-rigid 1DOF model

The Doherty-proposed semi-rigid 1DOF model has been used in practise. The mid-height acceleration-displacement curve for the rigid (blue dotted line) and semi-rigid model is depicted in Figure 5.2 (red line). The ultimate displacement (u) and the displacements (i) and (ii) in Fig. 5.2 are related to the material qualities and the state of deterioration of the mortar joints at the pivot locations, respectively. According to Sorrentino's proposed formulations (Sorrentino, 2003), the values of 1 and 2 have been assumed, and they are expressed in Eqns. 5.1 and 5.2.

$$\Delta_1 = 0.05 \cdot \Delta_u \quad (5.1)$$

$$\Delta_2 = 0.92 \cdot \Delta_1 + 0.21 \cdot \Delta_u \quad (5.2)$$

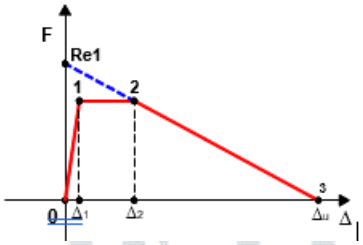

Fig.5.2 simply supported wall (1DOF model):mid-height acceleration-displacement curve

5.3.Gaussian inputs

Dynamic assessments of the set of walls have been conducted using Gaussian impulse inputs in terms of displacement with durations T1=1 s and T2=2 s and varied maximum amplitudes. In the 2DOF model, the stiffness Kd of the spring at the top has been taken into account for 4 different values: 1000 KN/m, 100 KN/m, 50 KN/m, and 10 KN/m. The displacement time-histories of wall n.1 for the 1DOF and 2DOF models are shown in Fig. 5.3 for Gaussian input with amplitude D=40 mm and T1=1 s: When Kd is increased, the response of the 2DOF model often replicates the response of

the top displacement s2 gets near to zero in the 1DOF model. The top displacement s2 grows as Kd decreases. The In the 1DOF model, rotations q1 and q2 that were in phase opposition become more uncoupled and autonomous. When Kd=10 KN/m is reached, the mid-height displacement s1 starts to decline after increasing from Kd=1000 KN/m to Kd=50 KN/m. When Kd is that number, top displacement s2 grows to be larger than mid-height displacement s1, then s2 and s1 start to phase with one another.

			Maximum displacement |Δ|max								
Wall	**Impulse duration**	**Impulse amplitude**	**1DOF**	**2DOF**							
				K_d=1000 KN/m		K_d=100 N/m		K_d=50 KN/m		K_d=10 N/m	
			s_1	s_1	s_2	s_1	s_2	s_1	s_2	s_1	s_2
		[m]	[m]	[m]	[m]	[m]	[m]	[m]	[m]	[m]	[m]
1	T_1=1 s	0,040	0,064	0,066	0,002	0,069	0,021	0,073	0,040	0,053	0,085
2	T_1=1 s	0,040	0,040	0,613	0,003	0,093	0,036	0,058	0,047	0,033	0,073
3	T_1=1 s	0,050	0,033	0,068	0,008	0,056	0,056	0,034	0,063	0,030	0,053

Table 5.2. Gaussian input: maximum mid-height and top displacements s_1 and s_2; comparison between 1DOFand 2DOF results

Table 5.2 shows the maximum displacements s_1 and s_2 of walls n.1, 2 and 3 for Gaussian impulse inputs with duration T_1=1 s and different amplitudes: the trend described for wall n.1 in Fig. 5.3 is

confirmed. Increasing the value of K_d the top displacement s_2 becomes close to zero, while the mid-height displacement s_1 increases until a specific value of K_d and then diminishes, so that s_2 becomes greater than s_1. With a significant overburden load (wall n.3) s_1 decreases while K_d gets smaller. The trend for Gaussian inputs with T_2=2 s is similar to the one with T_1=1 s.

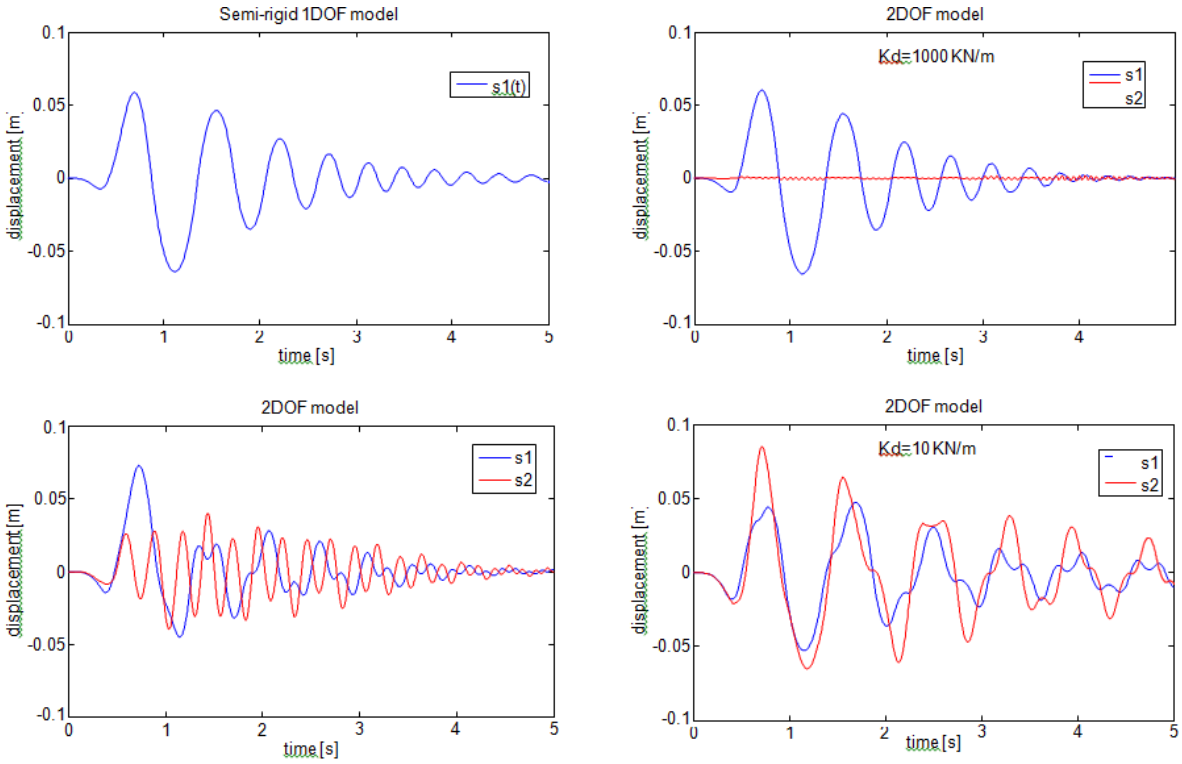

Fig.5.3 Wall n.1: displacement time-histories for 1DOF and 2DOF models with different values of K_d; s_1=mid-height displacement, s_2=top displacement; gaussian input with amplitude D=40 mm and duration T_1=1 s

5.4.Recorded accelerogram inputs

To conduct dynamic analysis on the three walls, 6 recorded accelerograms have been used as input. The properties of the records are described in Table 5.3.For the value of Kd = 500 KN/m, the response of the 2DOF model tends to reproduce the response of the 1DOF model, even better than for Gaussian inputs, as shown in Fig. 5.4, which scales the displacement time histories of wall n.1 for the El Centro record at 50% of PGA.

Table 5.3. Recorded accelerograms used in the analyses

Event	Year	Station	Id.	Component	PGA
Imperial Valley	1940	El Centro	Elce	S00E	0.348 g
Friuli	1976	Tolmezzo	tolm	270	0.315 g
Irpinia	1980	Sturno	stur	270	0.358 g
Loma Prieta	1989	Capitola	loma	000	0.529 g
Northridge	1994	Sylmar Hospital	Sylm	360	0.843 g
Kobe	1995	KJMA	kjmh	000	0.821 g

When Kd is decreased, the top displacement s2 grows and is significantly magnified at Kd=50 KN/m before becoming quite three times the value at Kd=500 KN/m. The top displacement s2 exceeds the mid-height displacement s1 for Kd=5 KN/m.

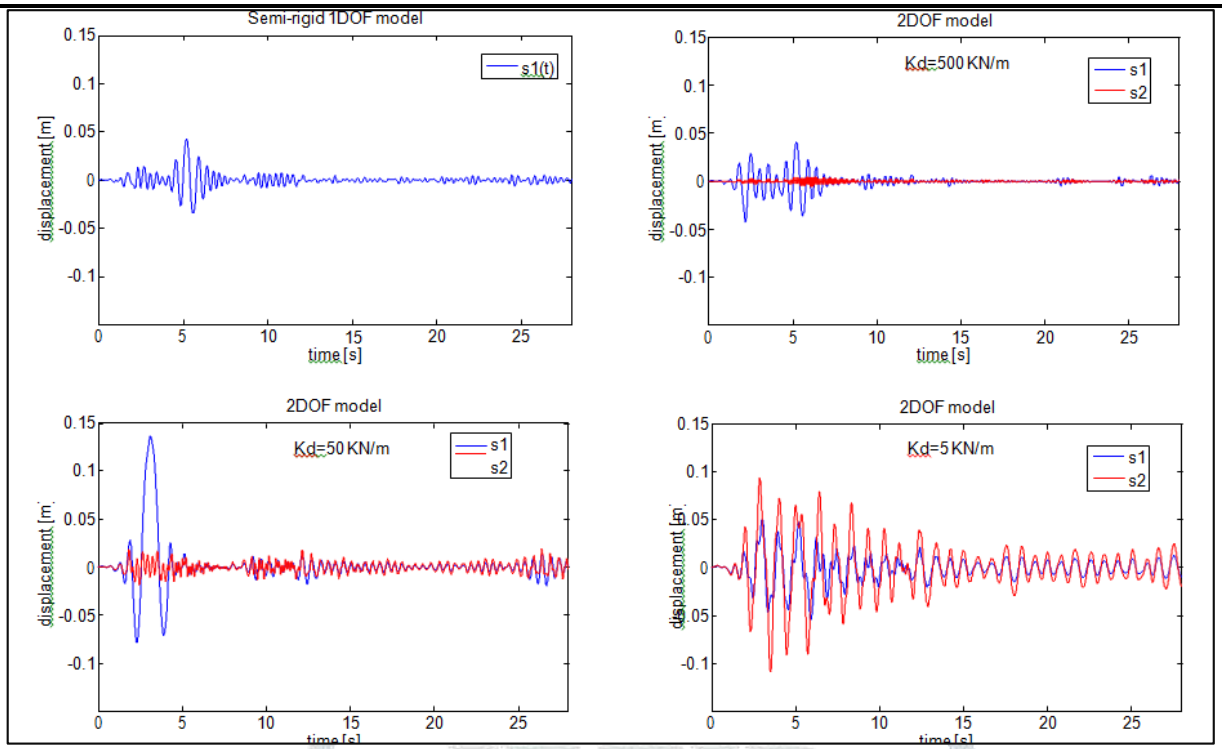

Figure 5.4 Wall n.1: displacement time-histories for 1DOF and 2DOF models with different values of K_d;s_1=mid-height displacement, s_2=top displacement; El Centro recorded accelerogram scaled to 50% of PGA

Table 5.4. Recorded accelerograms: maximum mid-height and top displacements s_1 and s_2; comparison between 1DOF and 2DOF results

Wall 1		**Maximum displacement |Δ|max**						
Accelerogram	**% PGA**	**1DOF**	**2DOF**					
			K_d=500 KN/m		K_d=50 KN/m		K_d=5 K/m	
		s_1 [m]	s_1 [m]	s_2 [m]	s_1 [m]	s_2 [m]	s_1 [m]	s_2 [m]
elce	50	0,043	0,043	0,004	0,137	0,019	0,050	0,109
tolm	100	0,094	0,094	0,004	0,114	0,036	0,048	0,095
stur	80	0,053	0,048	0,005	0,035	0,023	0,082	0,074
loma	50	0,031	0,034	0,004	0,039	0,026	0,056	0,078
sylm	35	0,045	0,047	0,005	0,057	0,028	0,077	0,082
kjmh	20	0,063	0,068	0,004	0,046	0,035	0,060	0,114

The maximum displacements s1 and s2 of wall n.1 for recorded accelerogram inputs scaled at various percentages of PGA are shown in Table 5.4; this partially confirms the trend shown in Fig. 5.4, even though it is less regular for various ground motions. The top displacement s2 approaches zero as Kd is increased, but the mid-height displacement s1 does not exhibit a consistent pattern across all samples. When Kd is high, the wall collapses due to an overwhelming demand for mid-height displacement, similar to how a simply supported wall (1DOF) collapses. Similar to a parapet wall, when Kd is small, s2 exceeds s1 and collapses due to an excessive demand for top displacement. Results for wall number two. and n. 3 are similar to the ones obtained for wall n. 1

5.5Observations

To more thoroughly evaluate the impact of diaphragm flexibility on the out-of-plane behaviour of walls, an expansion of the current study will be required. In any case, it is already conceivable to point out that, depending on the input and wall parameters, ignoring diaphragm flexibility might result in either an excessively cautious underestimating of the displacement demand on the wall or a considerable and dangerous overestimation. The displacement demand is actually greatly influenced by the diaphragms' flexibility, which makes it seem like a crucial parameter to take into account in dynamic assessments of the out-of-plane behaviour of unreinforced masonry walls.

6.CONCLUSIONS

The goal of the current work is to apply several formulations and ideas that have been previously put forth by other authors for the parapet wall and the simply supported wall to the case of out-of-plane bending of walls in structures with flexible diaphragms. Investigation of the results of dynamic analyses on a set of walls using recorded accelerogram inputs or Gaussian impulses revealed that the stiffness of the diaphragm significantly affects the displacement demand of the walls, despite the apparent impossibility of defining a general rule to predict such demand without conducting dynamic analyses. The model and numerical algorithm's underlying hypotheses need to be tested experimentally in order to be confirmed. Future advancements may include models of the inelastic behaviour of the spring at the top and the definition of a 3-degrees-of-freedom model that includes the in-plane walls.

REFERENCES

Doherty, K. (2000). An investigation of the weak links in the seismic load path of unreinforced masonry buildings. , PhD Thesis. Department of Civil and Environmental Engineering, The University of Adelaide.

Doherty, K., Griffith, M. C., Lam N. and Wilson, J. (2002). Displacement-based seismic analysis for out-of- plane bending of unreinforced masonry walls. *Earthquake Engineering and Structural Dynamics*, **31**, 833- 850

Griffith, M. C., Magenes, G., Melis, G. and Picchi, L. (2003). Evaluation of out of plane stability of unreinforced masonry walls subjected to seismic excitation. *Journal of Earthquake Engineering*, **7:S1**, 141-169

Griffith, M. C., Lam , N. T. K., Wilson , J. L. and Doherty, K. (2004). Experimental investigation of Unreiforced Brick Masonry Walls in Flexure. *Journal of Structural Engineering ASCE*. **130:3**, 423-432.

Housner, G.W. (1963). The behavior of inverted pendulum structures during earthquakes, *Bulletin of the Seismological Society of America*, **53:2**, 403-417.

Lam , N. T. K., Griffith, M. , Wilson, J. and Doherty, K. (2003). Time–history analysis of URM walls in out-of- plane flexure. Engineering *Structures*, **25**, 743-754

Simsir, C.C. (2004). Influence of diaphragm flexibility on the out-of-plane dynamic response of unreinforced masonry walls. PhD Thesis, University of Illinois at Urbana Champagne, Illinois, USA.

Sorrentino, L. (2003). Dinamica di muri sollecitati fuori del piano come sistemi di corpi rigidi. PhD Thesis, Dottorato di Ricerca in Ingegneria delle Strutture – XVI Ciclo Università degli Studi di Roma "La Sapienza"

Sorrentino, L., Masiani, R. and Griffith, M.C. (2008). The vertical spanning strip wall as a coupled rocking rigid body assembly, *Structural Engineering and Mechanics*, **29:4**, 433-453